Title

Discovery of Novel Activators of Large-Conductance Calcium-Activated Potassium Channels for the Treatment of Cerebellar Ataxia

Journal

Molecular Pharmacology, 102(1)

ISSN

0026-895X

Authors

Srinivasan, Sharan R

Huang, Haoran

Chang, Wei-Chih

et al.

Publication Date

2022-07-01

DOI

10.1124/molpharm.121.000478

Peer reviewed

1521-0111/102/1/17–28$35.00
MOLECULAR PHARMACOLOGY

dx.doi.org/10.1124/molpharm.121.000478
Mol Pharmacol 102:17–28, July 2022

Discovery of Novel Activators of Large-Conductance Calcium-Activated Potassium Channels for the Treatment of Cerebellar Ataxia[S]

Sharan R. Srinivasan, Haoran Huang, Wei-Chih Chang, Joshua A. Nasburg, Hai M. Nguyen, Tim Strassmaier, Heike Wulff, and Vikram G. Shakkottai

Brigham and Women's Hospital, Department of Neurology, Boston, Massachusetts (S.R.S.); University of Texas Southwestern Medical Center, Department of Neurology, Dallas, Texas (H.H., V.G.S.); University of Michigan, Department of Neurology, Ann Arbor, Michigan (S.R.S., W.-C.C.); University of California, Davis, Department of Pharmacology, Davis, California (J.A.N., H.M.N., H.W.); and Nanion Technologies, Munich, Germany (T.S.)

Received December 15, 2021; accepted April 7, 2022

ABSTRACT

Impaired cerebellar Purkinje neuron firing resulting from reduced expression of large-conductance calcium-activated potassium (BK) channels is a consistent feature in models of inherited neurodegenerative spinocerebellar ataxia (SCA). Restoring BK channel expression improves motor function and delays cerebellar degeneration, indicating that BK channels are an attractive therapeutic target. Current BK channel activators lack specificity and potency and are therefore poor templates for future drug development. We implemented an automated patch clamp platform for high-throughput drug discovery of BK channel activators using the Nanion SyncroPatch 384PE system. We screened over 15,000 compounds for their ability to increase BK channel current amplitude under conditions of lower intracellular calcium that is present in disease. We identified several novel BK channel activators that were then retested on the SyncroPatch 384PE to generate concentration-response curves (CRCs). Compounds with favorable CRCs were subsequently tested for their ability to improve irregular cerebellar Purkinje neuron spiking, characteristic of BK channel dysfunction in SCA1 mice. We identified a novel BK channel activator, 4-chloro-*N*-(5-chloro-2-cyanophenyl)-3-(trifluoromethyl)benzene-1-sulfonamide (herein renamed BK-20), that exhibited a more potent half-maximal activation of BK current (pAC50 = 4.64) than NS-1619 (pAC50 = 3.7) at a free internal calcium concentration of 270 nM in a heterologous expression system and improved spiking regularity in SCA1 Purkinje neurons. BK-20 had no activity on small-conductance calcium-activated potassium (SK)1–3 channels but interestingly was a potent blocker of the T-type calcium channel, Cav3.1 (IC_{50} = 1.05 μM). Our work describes both a novel compound for further drug development in disorders with irregular Purkinje spiking and a unique platform for drug discovery in degenerative ataxias.

SIGNIFICANCE STATEMENT

Motor impairment associated with altered Purkinje cell spiking due to dysregulation of large-conductance calcium-activated potassium (BK) channel expression and function is a shared feature of disease in many degenerative ataxias. BK channel activators represent an outstanding therapeutic agent for ataxia. We have developed a high-throughput platform to screen for BK channel activators and identified a novel compound that can serve as a template for future drug development for the treatment of these disabling disorders.

Introduction

Cerebellar degeneration is a cardinal feature of the ataxias, a group of disorders that result in balance impairment, speech changes, and oculomotor dysfunction (Durr, 2010; Shakkottai and Fogel, 2013). Neuronal dysfunction precedes cell loss and is more closely associated with motor impairment at symptom onset in a variety of murine models (Shakkottai et al., 2011; Dell'Orco et al., 2015, 2017; Chopra et al., 2018; Stoyas et al., 2019). Alterations in cerebellar Purkinje neuron spiking, the sole output of the cerebellar cortex, is a consistent early feature of disease in these models. Abnormal Purkinje neuron spiking is seen in models of the most common spinocerebellar ataxias (SCAs): SCA1, SCA2, SCA3, SCA6, and SCA7 (Shakkottai et al., 2011; Dell'Orco et al., 2015, 2017; Jayabal et al., 2016; Stoyas et al., 2019). The abnormal spiking is largely driven by potassium (K^+) channel dysfunction. In the SCAs that result in prominent loss of Purkinje cells, there is a progressive reduction in transcripts of large-conductance calcium-activated K^+ (BK)

This research was supported by National Institutes of Health National Institute of Neurological Disorders and Stroke [Grant R25-NS089450-06] (S.R.S.) and [Grant R01-NS085054] (V.G.S.) and by University of Michigan/Michigan Drug Discovery U069310 (S.R.S. and V.G.S.).

Tim Strassmaier is employed by Nanion Technologies, the manufacturer of the high-throughput patch clamp instrument SyncroPatch 384PE used in the current study. The authors declare that they have no conflicts of interest with the contents of this article.

dx.doi.org/10.1124/molpharm.121.000478.

[S] This article has supplemental material available at molpharm.aspetjournals.org.

ABBREVIATIONS: aCSF, artificial cerebrospinal fluid; AHP, afterhyperpolarization potential; APC, automated patch clamp; BK, large-conductance calcium-activated potassium; CRC, concentration-response curve; HEK, human embryonic kidney; HTS, high-throughput screen; ISI, interspike interval; NPC, Nanion patch clamp; QC, quality control; SCA, spinocerebellar ataxia; SK, small-conductance calcium-activated potassium.

channels (Dell'Orco et al., 2015; Chopra et al., 2018), an ion channel responsible for the afterhyperpolarization potential (AHP) that follows an individual action potential. The importance of BK channels in cerebellar health is illustrated by the development of profound cerebellar ataxia in BK channel knockout mice (Sausbier et al., 2004) and ataxia and cerebellar atrophy in humans with *KCNMA1* (gene that codes for BK channels) loss-of-function mutations (Liang et al., 2019; Miller et al., 2021). In SCA1 transgenic mice, restoring BK channel expression or compensating for the loss of the AHP rescues altered membrane excitability, improves motor dysfunction, and reduces Purkinje neuron degeneration (Chopra et al., 2018). Therefore, improving BK channel activity represents an attractive therapeutic strategy to restore Purkinje neuron impairment in degenerative ataxias.

BK channels are activated by both membrane depolarization and an elevation in intracellular calcium concentration. Prior efforts at development of BK channel activators have focused on agents for application in poststroke neuroprotection (Gribkoff et al., 2001; Huang et al., 2021). These agents allow greater BK current to activate in the presence of the high intracellular calcium expected in postischemic neurons. Studies in models of SCA1 (Chopra et al., 2020; Bushart et al., 2021), SCA2 (Chopra et al., 2020), and SCA7 (Stoyas et al., 2019) indicate, however, that inadequate activation of BK channels results from both reduced BK channel expression and reduced amounts of intracellular calcium needed to activate the channels during the interspike interval (Stoyas et al., 2019). This is supported by concomitant reduced expression of *Cacna1g* (Cav3.1, a T-type calcium channel) and *Itpr1* (the intracellular calcium channel, the inositol triphosphate receptor) that are potential calcium sources for BK channel activation. An important component of the spike in cerebellar Purkinje neurons is the AHP generated by BK and small-conductance calcium-activated potassium (SK) channels (Raman and Bean, 1999; Walter et al., 2006). Loss of the AHP is associated with irregular Purkinje neuron spiking, and this irregular spiking may be improved by activating SK channels (Walter et al., 2006). In a well characterized and genetically precise model of SCA1, $Atxn1^{154Q/2Q}$ mice (Watase et al., 2002), Purkinje neuron spiking is irregular due to a reduction in the amplitude of the AHP mediated by BK channels in association with reduced Cav3.1 expression. Although the irregular spiking in the $Atxn1^{154Q/2Q}$ mice and other SCA models may be improved by activation of SK (Kasumu et al., 2012; Bushart et al., 2021) and potentially Cav3.1 channels, we intended to focus on BK channel activators, as these channels are the root cause of the Purkinje neuron spiking abnormalities in models of the most common inherited ataxias. Moreover, activation of BK channels has the potential to slow neurodegeneration in a manner similar to restoring expression of *Kcnma1* (Chopra et al., 2018).

Traditionally, the analysis of physiologic properties of ion channels has relied on manual patch clamp, a reliable and highly specific but low throughput technique. Using a novel automated patch clamp (APC) instrument, the SyncroPatch 384PE, we designed a high-throughput screen (HTS) to explore and discover BK channel agonists that specifically enhanced current under conditions of low intracellular calcium. Hits from this primary screen were taken for concentration-response curves (CRCs) and followed up in cerebellar slice recording from the SCA1-KI mouse model.

We identified a compound, which we named BK-20, with greater potency against BK channels than NS-1619, a widely used tool-compound for BK channel activation (Olesen et al., 1994). Although inactive against small-conductance calcium-activated potassium (SK) channels, BK-20 was a potent inhibitor of Cav3.1. This work highlights the viability of APC for a neurodegenerative-focused HTS and offers a pharmacological probe of BK function and a lead molecule for further drug development.

Materials and Methods

APC Buffer Solutions

1. Potassium Sulfate Internal (0 mM Ca^{2+}): 84 mM K_2SO_4, 20.5 mM KCl, 10 mM EGTA, 10 mM HEPES, 1 mM $MgCl_2$, pH 7.4, 316 mOsm
2. Potassium Sulfate Internal (9 mM Ca^{2+}): 84 mM K_2SO_4, 2.5 mM KCl, 10 mM EGTA, 10 mM HEPES, 9 mM $CaCl_2$, 1 mM $MgCl_2$, pH 7.4, 307 mOsm
3. Barium External: 138 mM NaCl, 4 mM KCl, 5 mM $BaCl_2$, 5 mM dextrose, 10 mM HEPES, pH 7.2, 314 mOsm
4. 90% KF (Potassium Fluoride) Internal: 80 mM KF, 30 mM K-gluconate, 10 mM KCl, 10 mM NaCl, 10 mM HEPES, pH 7.4, 290 mOsm
5. 10× EGTA-Ca: 100 mM EGTA, 90 mM $CaCl_2$, pH 7.2
6. 10× EGTA-KCl: 100 mM EGTA, 180 mM KCl, pH 7.2
7. TEA Block: 40 mM NaCl, 100 mM TEA-Cl, 1 mM $MgCl_2$, 2 mM $CaCl_2$, 5 mM dextrose, 10 mM HEPES, pH 7.4
8. Extra Fill: 140 mM NaCl, 4 mM KCl, 5 mM dextrose, 10 mM HEPES, pH 7.4
9. External Standard: 140 mM NaCl, 4 mM KCl, 1 mM $MgCl_2$, 2 mM $CaCl_2$, 5 mM dextrose, 10 mM HEPES, pH 7.4
10. Seal Enhancer: 140 mM NaCl, 4 mM KCl, 1 mM $MgCl_2$, 4 mM $CaCl_2$, 5 mM dextrose, 10 mM HEPES, pH 7.4

SyncroPatch 384PE Patch Clamp, Multicell Mode, and Standard Whole-Cell Configuration

All cells were recorded in the whole-cell mode of the patch clamp technique using the SyncroPatch 384PE (Nanion Technologies, Munich, Germany). Electrophysiological protocols were constructed and data digitized using PatchControl 384 and DataControl 384 (Nanion Technologies). Using PatchControl 384, electrophysiological parameters such as seal resistance, capacitance, and series resistance were determined in each well after application of a test pulse and monitored over time throughout each buffer or compound administration.

Intracellular solution (6.33:3.67:90 10× EGTA-Ca:10× EGTA-KCl:90% KF Internal) for whole-cell recording was loaded into the intracellular compartment of a 384-well Nanion patch clamp (NPC) chip (Nanion Technologies). NPC chips were tested in one-, four-, and eight-hole formats as well as with low, medium, medium-plus, and high resistance features. Four-hole medium resistance NPC chips were used for both primary and secondary HTS after initial optimization steps (data not shown). All currents recorded are thus summations of the currents from the four individually captured cells within each well. Extra Fill solution was then loaded into NPC chip wells (30 μl/well). Trypsinized BK-HEK (human embryonic kidney) cell suspension (at least 400,000 cells/ml in External Standard solution) was pipetted into NPC wells (20 μl/well). Catch (−150 mbar for 5 seconds) and hold (−50 mbar for 30 seconds) pressures were applied to enrich cell capture. Seal Enhancer solution was then added to NPC wells (40 μl/well) to restore the final Ca^{2+} concentration to 2 mM. Fifty microliters per well was then removed and NPC wells were washed with External Standard (40 μl/well). Forty microliters per well was then

removed from each NPC well before proceeding to whole-cell configuration. After establishment of a whole-cell configuration, membrane currents were recorded using patch-clamp amplifiers in the SyncroPatch 384PE system.

Test compounds were applied to cells in NPC wells thereafter. Each application consisted of the addition of 40 μl of a 2× solution of compound into NPC wells for a final volume of 80 μl. Final solvent concentration was 0.1% DMSO, and final compound concentration was 10 μM in the primary screen. During concentration-response curve (CRC) generation, compounds were plated in duplicate at 2× in a titration such that final concentrations were 80 μM, 40 μM, 20 μM, 10 μM, 5 μM, 2.5 μM, 1.25 μM, and 0.625 μM. The duration of exposure to each compound was 3 minutes. After this, 40 μl was removed from each NPC well and 40 μl of blocking buffer (TEA Block) was administered with 2 minutes of subsequent recording.

Automated Patch Clamp: Voltage Dependence Protocols

Potassium currents were evoked with a step followed by a ramp voltage protocol. The voltage step was 300 milliseconds long from −90 to +100 mV, followed by a 1-second voltage ramp from −90 to +150 mV. Cells were maintained at a holding potential of −90 mV both before and between sweeps. Sweeps were applied every 10 seconds.

Automated Patch Clamp: Data Analysis

All initial APC data analysis and quality control (QC) were conducted using PatchControl 384 and DataControl 384 (Nanion Technologies). Wells that did not surpass a minimum seal resistance of 0.1 GΩ and baseline pretreatment current of >1 nanoampere (nA) were excluded and corresponding compounds were not included in primary screen log. Each compound was tested once in a single well. Wells in which interruptions of signal occurred were also excluded, including detachment of one or more of the four captured cells. Primary hits were identified as those compounds from wells passing aforementioned QC criteria resulting in a doubling of current post-treatment (as measured by $Peak_{Step}$). The Z' was defined as:

$$1 - \frac{3\,(\sigma_{NS-1619} + \sigma_{DMSO})}{\mu_{NS-1619} - \mu_{DMSO}}, \quad (1)$$

where μ was the mean and σ was the standard deviation. The Z' was monitored for each plate but was not used as a criterion for exclusion of plates from further analysis. IC_{50} values for concentration-response curves (CRCs) were calculated using GraphPad Prism.

Cerebellar Slice Electrophysiology

Patch clamp recordings were performed as previously described (Bushart et al., 2021). Briefly, mice were euthanized under deep isoflurane anesthesia, decapitated, and brains were placed in prewarmed (36°C) artificial cerebrospinal fluid (aCSF) bubbled with carbogen (95% O_2, 5% CO_2). The aCSF contained: 125 mM NaCl, 3.8 mM KCl, 26 mM $NaHCO_3$, 1.25 mM NaH_2PO_4, 2 mM $CaCl_2$, 1 mM $MgCl_2$, and 10 mM glucose. Parasagittal cerebellar sections were prepared in carbogen-bubbled aCSF at 33 to 35°C to 300 μM thickness using a vibratome (Leica Biosystems, Buffalo Grove, IL). Slices rested for 45 minutes before recording. For all patch clamp recordings, borosilicate glass pipets were pulled to 3 to 4 MΩ resistance and filled with an internal solution containing: 119 mM K-gluconate, 2 mM Na-gluconate, 6 mM NaCl, 2 mM $MgCl_2$, 0.9 mM EGTA, 10 mM HEPES, 14 mM Tris-phosphocreatine, 4 mM Mg-ATP, and 0.3 M Tris-GTP, at pH 7.3 and osmolarity 290 mOsm. Recordings were performed at 33 to 34°C in carbogen-bubbled aCSF at a flow rate of 2 to 3 ml/min 1 to 5 hours after slice preparation. Recordings were performed with an Axopatch 200B amplifier, Digidata 1440A interface, and pClamp-10 software (Molecular Devices, San Jose, CA). Data were acquired at 100 kHz and filtered at 2 kHz. Strict inclusion criteria were used for electrophysiological recordings. Purkinje neurons chosen for recording were morphologically identified as intact, teardrop shaped, and with no visible nucleolus or membrane blebbing. All neurons chosen for recording were noted to be spontaneously firing.

Electrophysiology data were processed and analyzed in ClampFit software (Molecular Devices, San Jose, CA). Spike regularity was measured as the coefficient of variation (CV) of the interspike interval (ISI), defined as (ISI standard deviation)/(ISI mean). Instantaneous firing rate and coefficient of variation of the interspike interval (CV ISI) were determined over 1 second of recording and binned to every minute for individual recordings.

Reagents: Cell Lines, Mouse Models, Buffers, and Compounds

Cell Lines. HEK-293 cells stably transfected with the BKα (pore-forming) subunit (BK-HEK) were a generous gift from Dr. Andrew Tinker and used by us previously (Villalobos et al., 2004; Kolski-Andreaco et al., 2007).

hSK1 and rSK2 were stably transfected into HEK-293 cells and were gifts from Khaled Houamed (University of Chicago) and Miao Zhang (Chapman University), respectively. hSK3 was stably transfected into COS7 cells by Aurora Biosciences (San Diego, CA; accession number AJ251015, cell line number 12124). Cav3.1 channels were stably expressed in HEK-293 cells (Kerafast, Boston, MA). All cells were cultured at 37°C, 5% CO_2, and 100% relative humidity in Dulbecco's Modified Eagle's Medium/Nutrient Mixture F-12 (DMEM/F12; Gibco) and supplemented with fetal bovine serum (FBS, 10% v/v), sodium pyruvate (0.5 mM; Gibco), penicillin-streptomycin (100 U/ml, 100 μg/ml), and geneticin (G418; 0.4 mg/ml). Of note, the cell lines used were not routinely checked for mycoplasma contamination.

Mice. All animal procedures were approved by the Institutional Animal Care and Use Committee (IACUC) at the University of Michigan and the University of Texas Southwestern Medical Center. $Atxn1^{154Q/2Q}$ knock-in mice were maintained on a C57Bl6J background (Jackson laboratories) by crossing $Atxn1^{154Q/2Q}$ males with $Atxn1^{2Q/2Q}$ wild-type females.

Chemical Library. The University of Michigan acquired a fraction of the chemical library from Dart Neuroscience, consisting of ~100,000 compounds with favorable characteristics for central nervous system drug applications, based on high blood-brain permeability, logP, number of rotational bonds, and molecular weight. We randomly selected compounds from this library, plated in 384-well plates, and tested over 15,000 compounds in our primary screen. For each 384-well compound plate, the first two columns (32 wells) were dedicated to DMSO control (plated at 0.2% for final concentration of 0.1%) and the final two columns (32 wells) were reserved for positive control compounds, NS-1619 (Tocris; plated at 100 μM in 0.2% DMSO for final concentration of 50 μM in 0.1% DMSO). Experimental compounds were plated at 2× at 20 μM in 0.2% DMSO for final working concentration of 10 μM in 0.1% DMSO in the primary screen. CRCs were conducted as a 2× titration from 80 μM over eight wells in duplicate. BK-4 (catalog number Z55879314), BK-5 (Z64811453), BK-19 (Z56759796), and BK-20 (Z45709388) were obtained from ENAMINE Ltd.

International Union of Pure and Applied Chemistry Nomenclature.

- NS-1619: 1,3-dihydro-1-[2-hydroxy-5-(trifluoromethyl)phenyl]-5-(trifluoromethyl)-2*H*-benzimidazol-2-one
- Chlorzoxazone: 5-chloro-3*H*-1,3-benzoxazol-2-one
- Baclofen: 4-amino-3-(4-chlorophenyl)butanoic acid
- BK-4: 5-(2-phenylquinolin-4-yl)-1,3,4-oxadiazole-2-thiol
- BK-5: 2-cyclopropyl-*N*-[4-(4-ethylpiperazin-1-yl)phenyl]quinoline-4-carboxamide
- BK-19: 4-[1-(4-hydroxyphenyl)-2-methylpropyl]phenol
- BK-20: 4-chloro-*N*-(5-chloro-2-cyanophenyl)-3-(trifluoromethyl)-benzene-1-sulfonamide

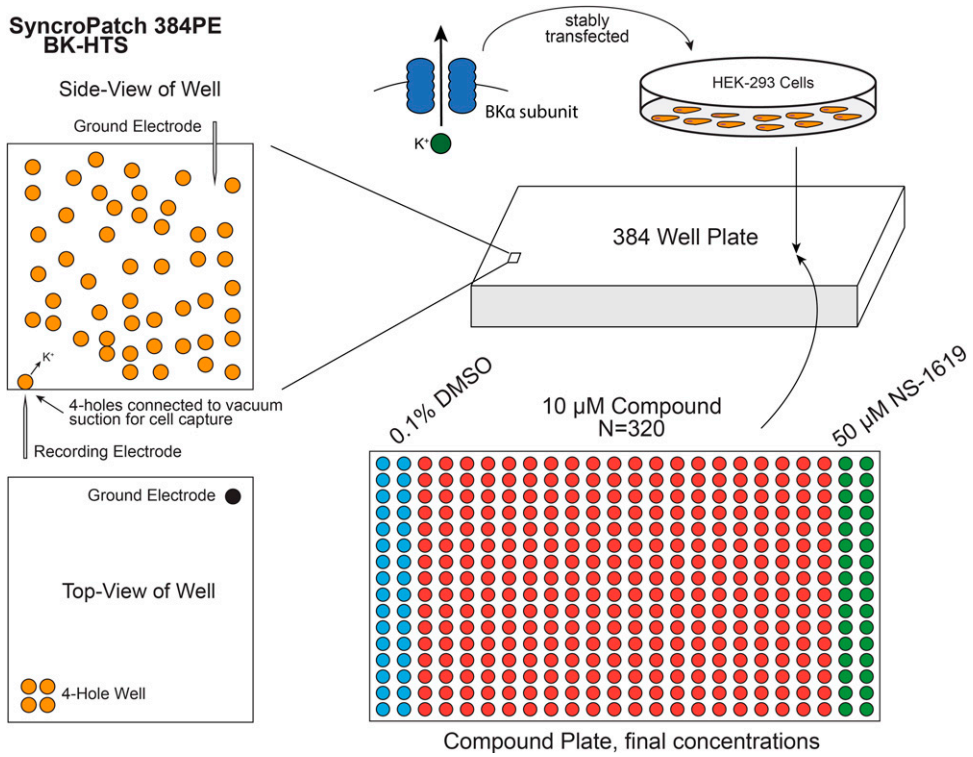

Fig. 1. Schematic of BK channel screen using SyncroPatch 384PE. HEK-293 cells stably transfected with the pore-forming α subunit of BK were seeded into the NPC-384 chip consisting of 384 wells. Four-hole chips with medium resistance were used. Vacuum suction was used to bring cells in contact with holes on the chip to form gigaohm seals and subsequently break the membrane for whole-cell recording. Compound plates were as designated, using the first two columns (32 wells) for DMSO control and final two columns (32 wells) for positive control (NS-1619).

Statistical Analysis

Statistical tests are described in the figure legends for all data. As this was an exploratory study, the null hypotheses were not prespecified and calculations for statistical power were not performed prior to study initiation. It follows from the exploratory nature of the experiments that calculated P values cannot be interpreted as hypothesis testing but only as descriptive. The data are expressed as mean ± S.D. unless otherwise specified. Sample size is included in each figure panel, either by plotting of individual data points or by including the number of cells (n) within the figure panel. pAC50 values indicated are calculated as $-\log(AC_{50})$, with AC_{50} values representing the half-maximal activation along a sigmoidal concentration-response curve. Data were analyzed using ClampFit 10.7 (Molecular Devices), MATLAB 2021b (MathWorks), GraphPad Prism 9 (GraphPad), SigmaPlot 14.5 (Systat), and Excel 2021 (Microsoft).

Results

Design and Optimization of a BK Channel High-Throughput Screen

Using the automated patch clamp instrument Nanion SyncroPatch 384PE, we designed a high-throughput screen to identify BK channel agonists (Fig. 1). In vivo, BK is comprised of the pore-forming alpha subunit and a complementary beta subunit that is often tissue-specific (Butler et al., 1993; Knaus et al., 1994; Brenner et al., 2000). In cerebellar Purkinje neurons, the β4 isoform is the predominant beta subunit that is expressed (Tseng-Crank et al., 1996; Brenner et al., 2000). There is, however, a discrepancy in the pharmacology of β4 containing BK channels expressed heterologously in cells versus the native BK channels in cerebellar Purkinje neurons. BKα/β4 expressed heterologously is insensitive to inhibition by iberiotoxin (Behrens et al., 2000; Meera et al., 2000), a selective inhibitor of BK channels. The AHP in Purkinje neurons is, however, sensitive to iberiotoxin, and iberiotoxin reproduces the changes in firing produced by knockout of *Kcnma1*, the BK channel gene (Sausbier et al., 2004). Since the goal of the current study was to augment BK currents in cerebellar Purkinje neurons, we used an alpha-subunit-only expressing BK channel stable cell line in HEK-293 cells (BK-HEK) that with manual patch clamp has previously been demonstrated to produce reliable, stable, and large-amplitude BK currents (Villalobos et al., 2004; Kolski-Andreaco et al., 2007).

To facilitate gigaohm seal formation with reliably high success on high-throughput automated patch platforms, it is necessary to have an internal/external solution pair that can form a precipitate at the interface between the external and internal solutions. We considered two options. The first option considered was an external barium chloride solution with an internal potassium sulfate solution. This allows barium sulfate to precipitate at the interface of the external and internal solutions to facilitate seal formation. The second option considered was to use a two-component KF-based internal solution. The first component of this solution would be a KF-based solution lacking Ca^{2+}. The second component would consist of a $CaCl_2$ solution with EGTA to buffer Ca^{2+} to the desired free Ca^{2+} concentration. The rationale for utilizing two separate components that are mixed immediately prior to use is that under equilibrium conditions, Ca^{2+} precipitates out of solution in the presence of fluoride and mixing the two components of the internal solution immediately prior to use delays the precipitation of CaF_2 out of the internal solution. A fluoride-containing

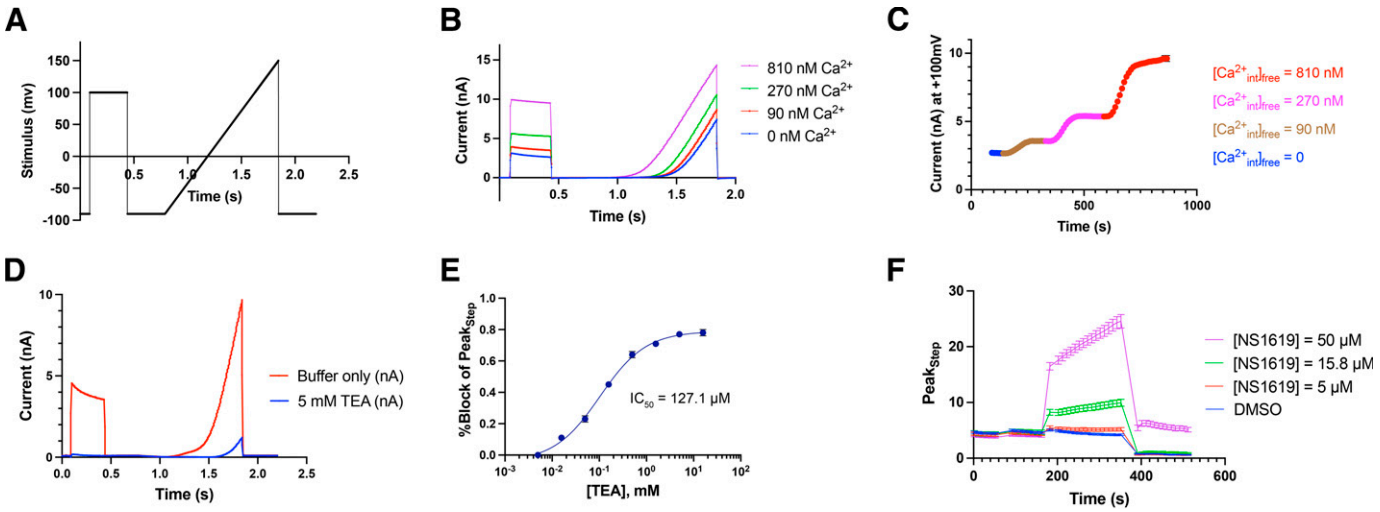

Fig. 2. Optimization of SyncroPatch 384PE conditions to identify a BK channel activator. Currents from BK-HEK cells were measured on the SyncroPatch 384PE to assess conditions and viability for a high-throughput screen. All currents shown are summations of four cells captured in each well. (A) A voltage step was applied to +100 mV from a holding potential of −90 mV, followed by a voltage ramp from −90 mV to +150 mV to evoke BK currents. (B) Overlaid traces from four different wells recorded using four different internal solution calcium concentrations. BK current activation is dependent on free calcium concentration in the internal solution and maximal with 810 nM internal solution free Ca^{2+} concentration. Current activation with a voltage ramp demonstrates the characteristic outwardly rectifying BK current with activation of current at more hyperpolarized membrane potentials at the highest calcium concentration. (C) BK currents are sensitive to internal calcium concentrations in a dose-dependent manner. Time course of $Peak_{Step}$ current after exchange of internal solution containing increasing concentrations of free calcium. (D) BK current at 810 nM internal solution free calcium is blocked by tetraethylammonium (TEA), summarized in the concentration-response curve in (E). (F) Calcium-dependent current can be stimulated by NS-1619, though only at high concentrations. For the purposes of HTS, 50 μM NS-1619 was used as the positive control.

internal solution facilitates gigaohm seal formation as the high calcium concentration of 2 mM Ca^{2+} in the external solution readily causes precipitation of CaF_2 at the interface between the internal and external solution.

With a barium external/K^+ sulfate internal solution combination, using eight-hole chips, we could record large BK currents. The seal rate was, however, only 42% (not shown). Comparatively, the seal rate using our two-component KF-internal and buffered calcium solution was excellent at 93%. With the two-component buffering system, BK currents activated by 810 nM free Ca^{2+} in the internal solution were stable for up to 2.5 hours (not shown), suggesting the stability of free calcium concentration up to 810 nM using this fluoride-based internal solution. In this system, free Ca^{2+} greater than 810 nM could not be achieved with a KF-based internal solution, as this is the practical Ca^{2+} buffering limit of EGTA. Recent buffer modifications with lower affinity chelators do allow for achieving up to 12 μM of free Ca^{2+} (data not shown). We determined the calcium responsiveness of BK currents with this solution by adjusting the free Ca^{2+} concentration to a range between 90 and 810 nM. BK currents were evoked with a depolarizing voltage step to +100 mV from a holding potential of −90 mV, followed by a 1-second voltage ramp between −90 and +150 mV (Fig. 2A). Initially, solutions with discrete free Ca^{2+} concentrations were used to evoke currents in different cells (Fig. 2B), with a clearly greater current amplitude in cells in which currents were evoked using a higher free Ca^{2+} concentration of 810 nM. To more directly demonstrate Ca^{2+} responsiveness of current amplitude, we performed internal solution exchange (Fig. 2C). The BK channel current amplitude increased with successive exchange of internal solution containing a free Ca^{2+} concentration of 90 nM, 270 nM, and 810 nM. The peak somatic Ca^{2+} concentrations in healthy Purkinje neurons with spontaneous spiking rates of 25–125 Hz varies from 80 to 320 nM (Womack et al., 2009). As the baseline BK current at 90 nM at an internal free Ca^{2+} concentration was small, we chose to perform the HTS at a 270-nM internal free Ca^{2+} concentration, as this provided reliable currents and is in the range of internal free Ca^{2+} concentration present in cerebellar Purkinje neurons (Womack et al., 2009). To demonstrate that the BK currents evoked through this protocol exhibited appropriate pharmacology, we examined the effect of external tetraethylammonium (TEA) for its ability to block BK currents with an internal calcium concentration of 810 nM, a free calcium concentration at which the residual delayed-rectifier current native to HEK-293 cells is a small proportion of the total current. BK currents were inhibited in a dose-dependent fashion by external TEA (Fig. 2D), with an inhibition constant (IC_{50}) of ~127 μM (Fig. 2E), characteristic of BK channels. NS-1619, a widely used tool compound for BK channel activation (Olesen et al., 1994; Gribkoff et al., 2001), increased BK current amplitude on the SyncroPatch 384PE platform. At the free Ca^{2+} concentration of 270 nM used in the HTS, NS-1619 was largely ineffective at concentrations below 15 μM and required higher concentrations for reliable BK current activation (Fig. 2F). We thus chose 50 μM NS-1619 as our positive control for the HTS, as this was the highest concentration soluble in our assay buffer.

Our goal from the screen was to identify an agent that would activate BK channel current and thereby modify cerebellar Purkinje neurons spiking. DMSO was used as a vehicle to dissolve compounds for testing and by itself had no effect on the BK current (Fig. 3, A and B). As above, NS-1619, (Olesen et al., 1994; Gribkoff et al., 2001) at a concentration of 50 μM, was included as a positive control (Figs. 2D;

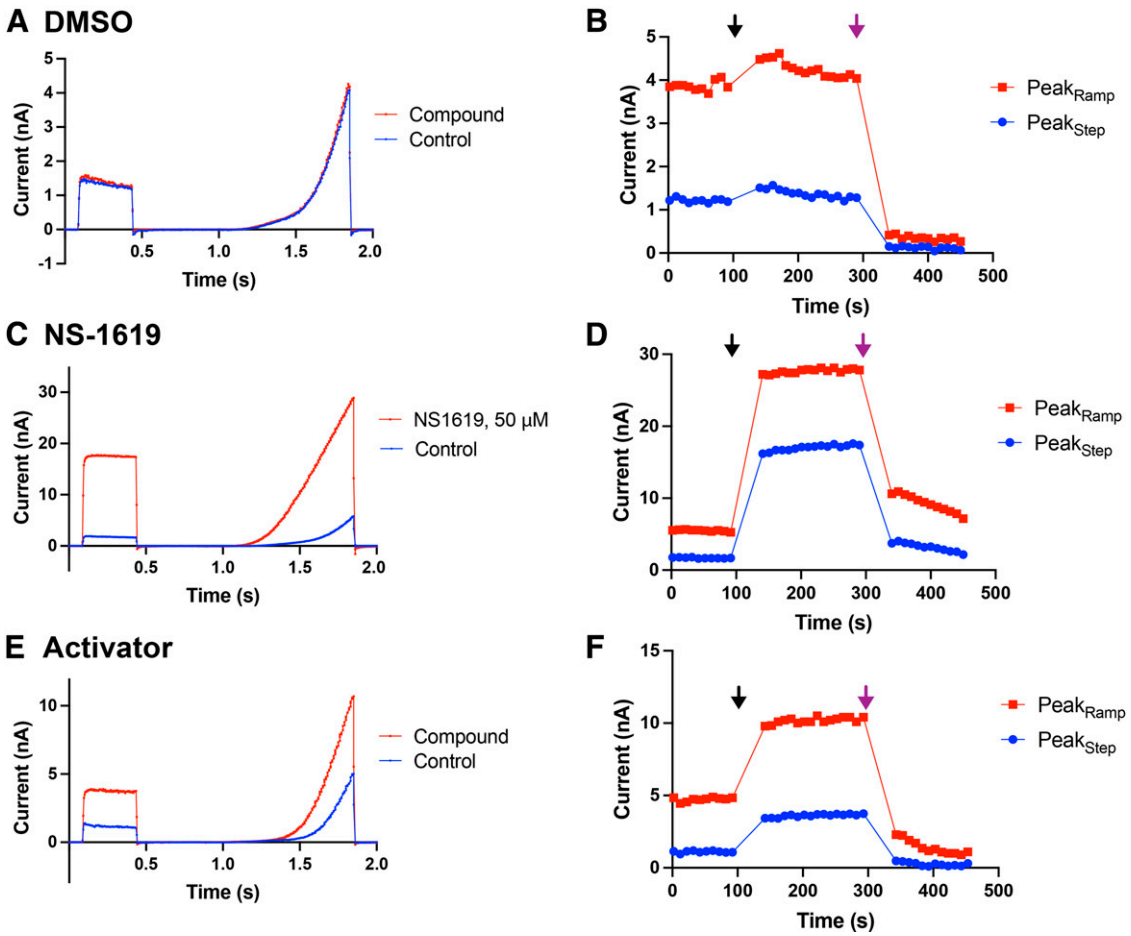

Fig. 3. High-throughput screen for BK channel modulators on the SyncroPatch 384PE platform. Current traces were recorded for 100 seconds (reference trace) prior to administration of compound. For each compound, the left panel (A, C, and E) shows the current in response to step-ramp voltage stimulus, whereas the right panel (B, D, and F) shows $Peak_{Step}$ and $Peak_{Ramp}$ over time. (A and B) DMSO (at 0.1%), the vehicle for the compounds in the screen, had no effect on the current. (C and D) Fifty micromolar NS-1619 increased current amplitude and markedly shifted the voltage dependence for current activation to more negative membrane potentials. (E and F) Illustration of the scheme for recognizing BK current activation by 10 μM of a compound from the Dart library. Compounds were advanced to repeat testing and concentration-response curves (CRCs) if there was at least a doubling in $Peak_{Step}$ current from reference. Note that this compound did not succeed in CRCs. Black arrow: administration of 10 μM compound. Purple arrow: administration of 50 mM TEA block.

3, C and D). A blocking step with TEA was included to evaluate reversibility of compound effect. The Z' was monitored for each plate but was not used as a criterion for exclusion of plates. The primary HTS Z' scores over the 55 primary screen plates ranged from −0.27 to 0.76, with a mean of 0.2 and median of 0.22 (Supplemental Material). Activators were identified by the increase in peak current in the step depolarization and peak of the ramp depolarization (Fig. 3, E and F). Although not the intent of our screen, we also identified many potent BK channel blockers (data not shown), some of which may have applications in other disease states.

Primary and Secondary Screens

We screened over 15,000 compounds from the Dart Therapeutics chemical library. A portion of this library was purchased by the University of Michigan. Dart Therapeutics, now defunct, had designed a large library primed for central nervous system activity based on various chemical parameters, including molecular weight, logP, number of rotational bonds, solubility, and predicted blood-brain permeability. Of the over 15,000 compounds that we tested in our initial primary screen, we identified 20 that met criteria (at least a doubling of current measured by $Peak_{Step}$ and seal resistance >100 MΩ per well) for advancing to secondary concentration-response curves (CRCs). This low hit rate (0.13%) demonstrates the challenges of identifying BK channel activators through more traditional means, including lower-throughput patch clamp methods, and demonstrates the value of the SyncroPatch 384PE instrument for such a high-throughput screen. CRCs on the 20 compounds were performed in duplicate with similar recording parameters as the primary screen. Fifty micromolar NS-1619 again served as a positive control. Of the 20 compounds tested, four demonstrated clear BK channel activation in the CRCs with pAC50s all greater than 3. However, BK-20 (Fig. 4G) appeared to be the only compound that qualitatively improved current activation more at higher concentrations compared with NS-1619 (Fig. 4H). Two others, BK-4 (Fig. 4, A and B) and BK-19 (Fig. 4, E and F) had superior pAC50 values to NS-1619 (4.53 vs. 3.70 and 5.30 vs. 3.70, respectively) but qualitatively elicited similar current activation to NS-1619 at the highest tested concentration. Overlaid step-ramp traces demonstrate that 50 μM NS-1619 augments BK current to a similar amplitude as

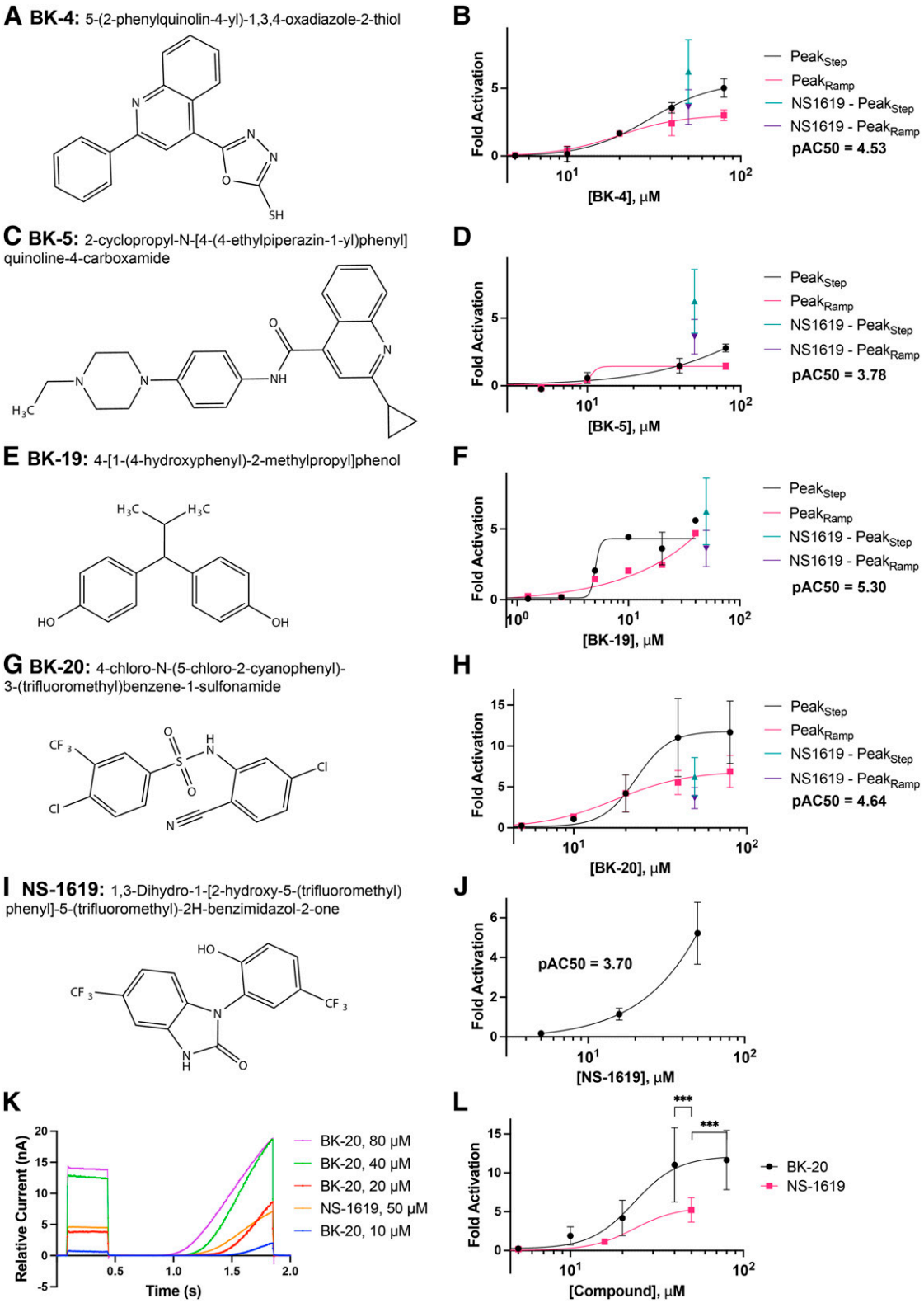

Fig. 4. Concentration-response curves (CRCs) for the four compounds that displayed activation of BK current. Compounds BK-4, BK-5, BK-19, BK-20, and NS-1619 were tested for concentration dependence of BK current activation on the SyncroPatch 384PE platform in duplicate. Structures for experimental compounds and NS-1619 are shown on the left (A, C, E, G, and I) with concentration-response curves on the right (B, D, F, H, and J). BK-4 and BK-5 that shared a quinolone (azanaphthalene benzopyridine) (A and C) were less effective in activating BK current than NS-1619 at all concentrations tested. Forty micromolar of compound BK-19 (E) activated BK current similar to 50 μM NS-1619, though both 80-μM wells did not pass QC metrics (F) and so were not included in the comparative analysis. (G) BK-20 qualitatively exhibited superior current activation when overlaying step-ramp traces with NS-1619 (K). Each concentration of BK-20 is shown as an average of duplicate, whereas NS-1619 is an average of 16 wells. Due to poor solubility of NS-1619 at a concentration of >50 μM, CRC curves for BK-20 (H) and NS-1619 (J) could not be directly compared (L). However, both 40 μM and 80 μM BK-20 activated significantly more current than 50 μM NS-1619, with statistical significance assessed by a two-tailed t test. Notably, both BK-20 and NS-1619 share a trifluoromethyl benzene group. All traces are normalized to pretreatment control currents. *** = $P < 0.001$.

20 μM BK-20 (Fig. 4K), whereas higher concentrations of BK-20 elicited even more current. Due to limited solubility of NS-1619, we were unable to directly compare the concentration-response curves of NS-1619 (Fig. 4J) and BK-20 to account for the greatest current activation seen at the highest concentrations of BK-20 (Fig. 4L). The current activation of BK-20 at the highest tested concentrations of 40 μM and 80 μM were each significantly greater than the current activation achieved by the highest tested concentration of 50 μM NS-1619.

Cerebellar Slice Recordings

Unlike imaging or radioisotope-flux based screens, the SyncroPatch 384PE allows for direct measurement of current. Since we had established current augmentation through the CRCs, we directly proceeded with examining the ability of identified compounds for the target application, namely improvement in firing of cerebellar Purkinje neurons in a murine model of SCA1. We tested NS-1619 and all four compounds with favorable CRCs (BK-4, BK-5, BK-19, and BK-20) for their ability to improve irregular Purkinje neuron spiking in cerebellar slices from *Atxn1*$^{154Q/2Q}$ mice. Purkinje neurons in *Atxn1*$^{154Q/2Q}$ mice display irregular spiking because of reduced BK channel expression and activity (Bushart et al., 2021). An increase in the coefficient of variation of the interspike interval (CV ISI) quantifies the degree of spiking irregularity in these neurons. BK-4, BK-5, BK-19, and BK-20 were perfused at 10 μM to examine their ability to improve spiking irregularity and alter firing rate. Although all four BK compounds were more active at higher concentrations, we chose to monitor improvement in Purkinje neuron physiology in cerebellar slices from *Atxn1*$^{154Q/2Q}$ mice at 10 μM, as we felt that if the compound was poorly active or inactive at this concentration, it was unlikely to serve as a useful scaffold for future drug development. Instantaneous firing rates (FR) and CV ISI (or just CV) were examined and compared with the baseline firing properties. Notably, NS-1619 failed to improve the CV ISI at 10 μM, only improving it at 50 μM (Fig. 5A). Similarly, compounds BK-4, BK-5, and BK-19 failed to alter Purkinje neuron CV ISI at a concentration of 10 μM (Fig. 5, B–D).

BK-20, the most active of the four compounds identified in the primary screen, showed clear ability to alter Purkinje neuron spiking in cerebellar slices from *Atxn1*$^{154Q/2Q}$ mice at a concentration of 10 μM. At baseline, Purkinje neurons in *Atxn1*$^{154Q/2Q}$ mice demonstrate irregular spiking (Fig. 6A). After perfusion of BK-20 (Fig. 6B), there is significant improvement in irregularity of spiking and an increase in Purkinje neuron firing frequency (summarized in Fig. 6, C and D). Consistent with its likely internal binding site for BK channels, BK-20 could not readily be washed out (Fig. 6C). Although some of the SCA1 Purkinje neurons tested had only modest spiking irregularity in the current study, the magnitude of improvement in spiking irregularity is similar to what was achieved previously with a combination of baclofen and chlorzoxazone, drugs that also improved motor impairment in these SCA1 mice (Bushart et al., 2021).

Target Validation

We next sought to determine if the effects of BK-20 on Purkinje neuron spiking in *Atxn1*$^{154Q/2Q}$ mice were truly mediated by effects on BK and not by other channels that can improve the irregular firing phenotype without addressing the root cause of reduced BK channel expression. In addition to reduced *Kcnma1*, *Atxn1*$^{154Q/2Q}$ mice show decreased expression of the T-type calcium channel *Cacna1g* (Cav3.1), and activation of this current by BK-20 could be postulated to improve irregular spiking (Stoyas et al., 2019; Chopra et al., 2020). Further, SK channel activators have been shown to ameliorate the irregular firing phenotype in SCAs (Kasumu et al., 2012).

BK-20's activity was therefore tested against all three SK channels (SK1, SK2, and SK3) as well as Cav3.1. BK-20 at 10 μM had no effect on any of the heterologously expressed SK channels (Fig. 7), whereas NS309, a known SK channel activator (Strøbæk et al., 2004) that served as a positive control, showed robust SK channel current activation at a similar concentration (Fig. 7, A and B). Unexpectedly, BK-20 potently inhibited Cav3.1 (Fig. 7, C and D), with an IC_{50} of 1.05 μM. Nevertheless, these results confirm that the improvement in firing seen in *Atxn1*$^{154Q/2Q}$ mice with BK-20 is due to its activity on BK instead of other channels. These results also confirm our prior data that increasing BK channel activity is sufficient to improve irregular spiking even in the presence of reduced Cav3.1 expression (Stoyas et al., 2019), the activity of which is likely reduced further by BK-20.

Discussion

In this study, we implement an APC platform to identify a novel activator of the large-conductance calcium- and voltage-gated BK channel. BK channel dysfunction is a feature of disease in a variety of models of cerebellar ataxia, and restoring BK channel expression both improves motor dysfunction and delays degeneration (Chopra et al., 2018). In models of ataxia, in addition to loss of BK channels, there is a reduction in expression of potential Ca^{2+} sources for BK channel activation (Stoyas et al., 2019; Chopra et al., 2020; Bushart et al., 2021). Targeting the irregular spiking that results from a reduction in the BK channel AHP improved Purkinje neuron firing and motor impairment in the genetically precise and well characterized *Atxn1*$^{154Q/2Q}$ model (Watase et al., 2002) of SCA1 used in the current study (Bushart et al., 2021). Previous attempts to develop BK channel activators for therapeutic use have focused on identifying agents that increase current in the presence of high intracellular calcium. We attempted to identify BK channel activators that would augment current in the presence of low intracellular Ca^{2+}, a necessity to target impaired cerebellar Purkinje neuron spiking in SCAs.

Ion channels represent a major target for neurologic disease and constitute a large fraction of currently approved neuropharmaceuticals. Unfortunately, developing novel compounds against ion channels has proven to be an arduous task, in part due to technical limitations. Rational design suffers from transmembrane structural ambiguities and difficulty in expressing and purifying such proteins in vitro. Major strides in cryo-EM (cryo-electron microscopy) and crystallography have improved our

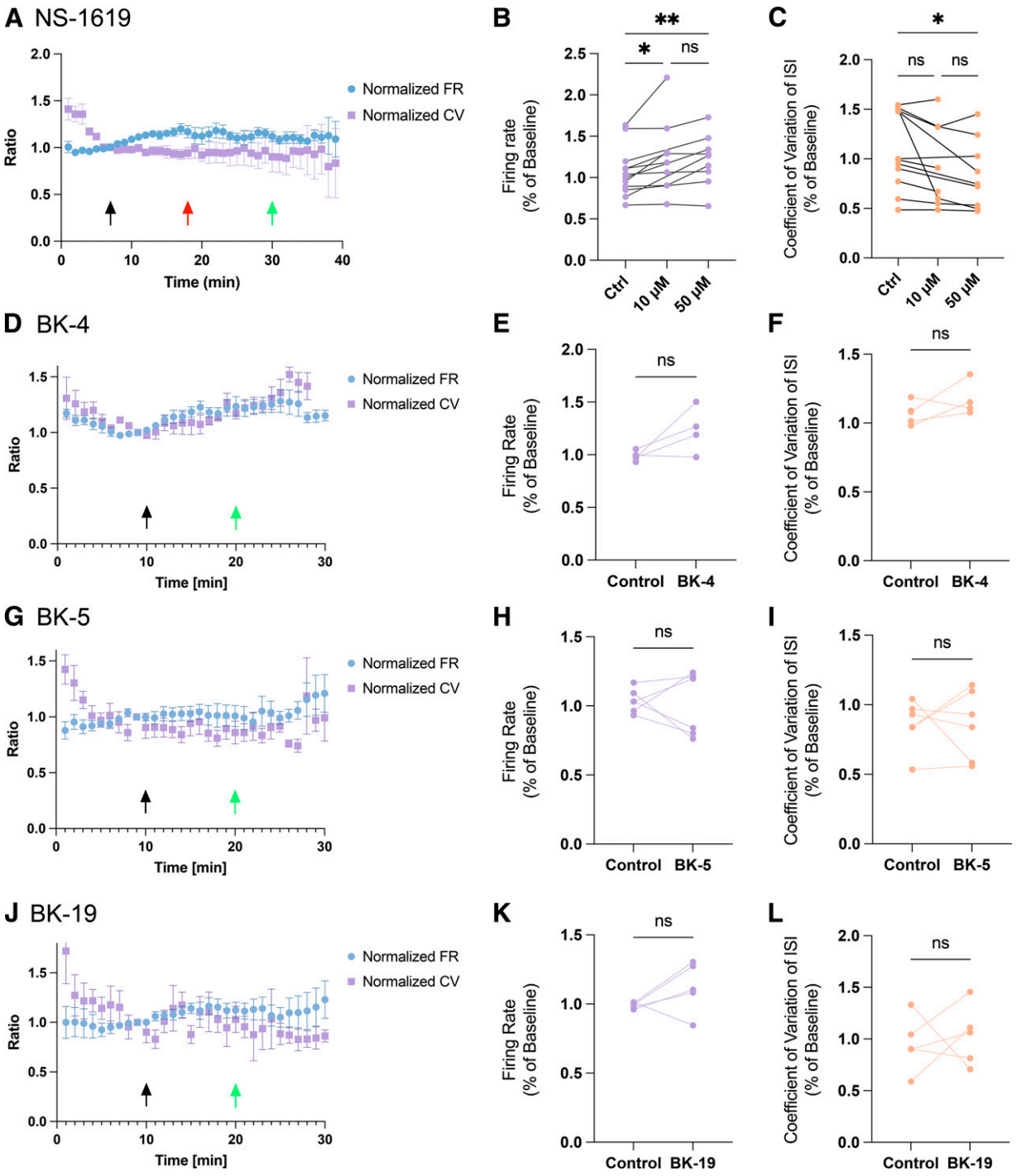

Fig. 5. Cerebellar slice recordings in SCA1 mice to determine ability of compounds identified in the screen to improve irregular Purkinje neuron spiking. BK-4, BK-5, and BK-19 exhibited BK current activation similar to or less than NS-1619 and were tested for their ability to modify the abnormal Purkinje neuron spiking in cerebellar slices from *Atxn1*$^{154Q/2Q}$ (SCA1 knock-in) mice. Compounds were perfused after 10 minutes with a washout at 20 minutes after 10 minutes of on-drug recording. (A) NS-1619 was tested for its ability to modify Purkinje neuron spiking at a concentration of 10 μM (n = 8) and 50 μM (n = 9) and normalized to the baseline firing in each cell. Fifty micromolar NS-1619 increased firing rate and improved spiking irregularity, summarized in (B) and (C), respectively. (D) BK-4 (n = 6) failed to significantly improve firing rate or firing irregularity at 10 μM, summarized in (E) and (F), respectively. (G) BK-5 (n = 6) failed to significantly improve firing rate or firing irregularity at 10 μM, summarized in (H) and (I), respectively. (J) BK-19 (n = 5) failed to significantly improve firing rate or firing irregularity at 10 μM, summarized in (K) and (L), respectively. Statistical analysis was performed by comparing equilibrium firing rate CV ISI prior to and after drug infusion at 10 minutes using Student's t test. For NS-1619, a two-way ANOVA was used with timepoints 7 minutes (10 μM) and 18 minutes (50 μM). * = $P < 0.05$, ** = $P < 0.01$. Black arrow: administration of 10 μM drug; red arrow: 50 μM drug; green arrow: washout.

structural understanding of ion channels, particularly in the dynamic state, but rational development solely using structure-based design remains difficult. Manual patch recording of cells or brain slices, although highly dynamic and reliable, is extremely low throughput and restricts the number of chemical scaffolds that can be tested.

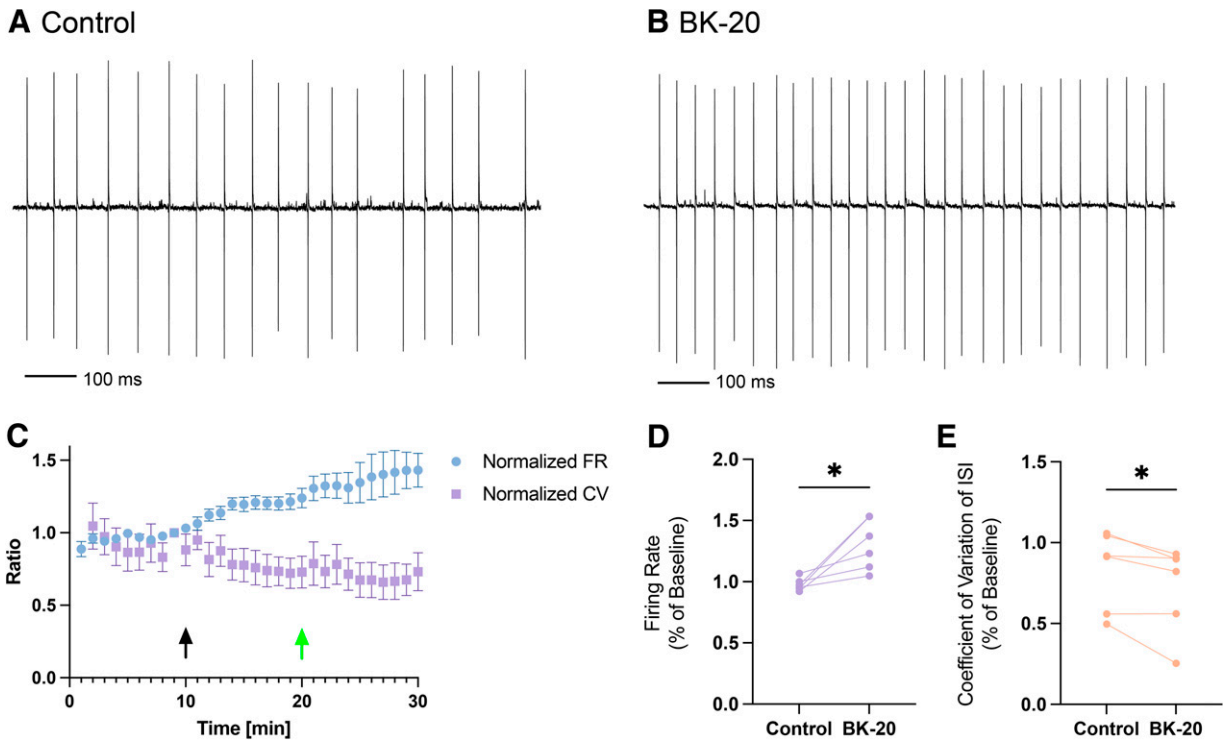

Fig. 6. BK-20 improves the aberrant spiking in SCA1 mice. BK-20 exhibited greater current activation than NS-1619 at the highest concentration tested of each compound and was tested for its ability to modify the abnormal Purkinje neuron spiking in cerebellar slices from *Atxn1*$^{154Q/2Q}$ (SCA1 knock-in) mice. (A) Baseline recording of Purkinje neuron spiking in SCA1 mice showing irregular spiking. (B) After perfusion of BK-20 at 10 μM ($n = 8$) there is an increase in firing frequency and the regularity of spiking; timeline of changes in firing properties is summarized in (C). BK-20 significantly increased firing rate (D) and decreased the CV ISI (E) of Purkinje neuron spiking in SCA1 mice. Statistical analysis was performed by comparing equilibrium firing rate and CV ISI prior to and after drug infusion at 10 minutes using Student's t test. * = $P < 0.05$. Black arrows: administration of 10 μM drug; green arrow: washout.

Thallium flux assays have been used to develop HTS for ion channels, as thallium can permeate potassium channels and thereby act as a charge carrier for K^+ channels (Weaver et al., 2004; Weaver, 2018). Designing such a thallium-flux assay for calcium-activated potassium channels is, however, challenging. Also, secondary screens are needed to directly measure currents and examine whether current augmentation occurs. APC provides a unique and powerful platform for analyzing ion channel activity with high throughput. We developed an APC HTS to directly measure BK current with an intracellular Ca^{2+} concentration most relevant to our application of augmenting current in cerebellar Purkinje neurons. Although we were able to examine over 15,000 compounds, this represents only a fraction of potential chemical scaffolds to be examined. Further investigation of larger compound sets yielding additional molecular skeletons will guide future structure-activity relationship studies.

An APC HTS requires a precipitate to form at the interface of the internal and external solutions. Conventionally, the precipitate is an insoluble calcium salt, making it challenging to develop such a screen for calcium-activated potassium channels. Using a two-component buffer system and keeping the free Ca^{2+} low in the internal solution enabled us to design an HTS to identify novel activators of BK current. In our screen, the precipitation of calcium and fluoride at the interface between the external and internal solutions increases seal rates to over 90%, with a resistance of >0.4 GΩ, without affecting the stability of the recorded BK current or precipitation of calcium in the internal solution up to a free calcium concentration of 810 nM. Although the Z' for the primary HTS was somewhat low (average of 0.2 over 55 plates), there was an increase over the course of the screen (Supplemental Material), suggestive of the importance of user experience with the instrument. Further, increased variability in the degree of BK current activation and the relatively modest current activation by NS-1619 even at 50 μM led to this relatively low Z' score, as there was little BK current activation or variability of current activation with DMSO (negative control). Improvement of the Z' could be achieved in a future BK HTS using a positive control such as BK-20 or a chemogenetic model, given the variable current activation with NS-1619. Because we chose to define a primary hit based on relative current change from pretreatment instead of a percentage of positive control signal, we were able to minimize the false discovery rate. Despite screening over 15,000 compounds, we only identified 20 primary hits. This low hit rate speaks to the specificity of our assay and suggests a higher percentage of hit validity. Four of the 20 compounds succeeded in reproducing BK current augmentation for CRCs, with two achieving qualitatively similar current activation as NS-1619. A validation rate of 10%–20% exceeds most conventional HTS platforms.

Purkinje neuron spiking irregularity in *Atxn1*$^{154Q/2Q}$ mice has been addressed using a combination of chlorzoxazone-baclofen (10 μM–400 nM) without negatively impacting firing rate (Bushart et al., 2021). Interestingly, neither chlorzoxazone nor baclofen alone at these concentrations was able to improve the regularity of Purkinje

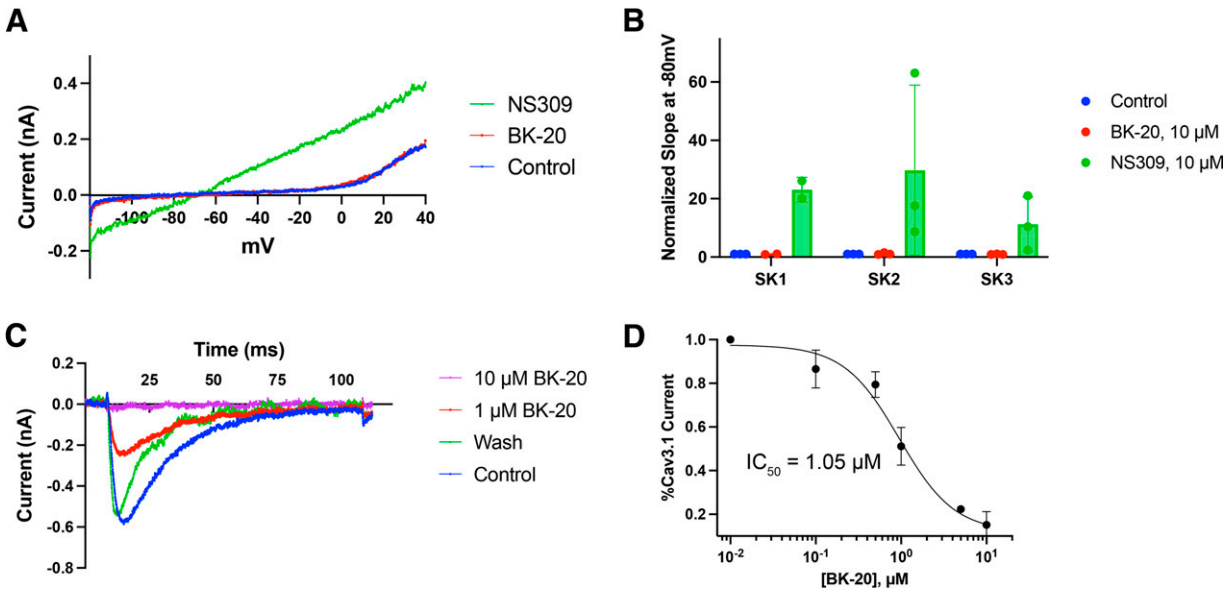

Fig. 7. BK-20 is inactive against SK channels but inhibits Cav3.1. BK-20 was tested for its ability to activate SK1, SK2, SK3, and Cav3.1 channels. Currents were elicited in heterologously expressed channels using manual patch clamp. (A) Sample trace of SK2 current, the predominant SK channel isoform in Purkinje neurons, in the presence of 250 nM free calcium in the internal solution. NS309, a known SK channel activator, demonstrates a robust activation of current, whereas BK-20 has no effect. (B) Comparison of BK-20 and NS309 effects across on SK1, SK2, and SK3, demonstrating lack of effect of BK-20 on any SK channel. (C) Concentration dependence of inhibition of Cav3.1 by BK-20. Inhibition of Cav3.1 by BK-20 is reversible. (D) Concentration-response curve for BK-20 against Cav3.1 demonstrates that it is a potent antagonist.

neuron firing. These agents do not target BK channels directly (Bushart et al., 2018), however, and have not been demonstrated to slow Purkinje neuron degeneration. Since BK channels are the root cause of Purkinje neuron dysfunction and degeneration, an agent augmenting BK channels directly is more likely to both improve motor impairment and slow degeneration (be neuroprotective). Further, combinatorial strategy increases risk of polypharmaceutical adverse effects as compared with using a drug with a single target.

Monogenic neurodegenerative diseases have emerged as an area of significant interest for development of gene-specific therapy. Although gene-specific therapy is an attractive option for preventing disease progression in SCAs, it is apparent that downstream nodes of dysfunction, such as irregular Purkinje spiking, drive both motor symptoms and cerebellar degeneration and are also therefore attractive targets for intervention. Correction of irregular/aberrant Purkinje neuron spiking through targeting ion channels distinct from BK channels can be effective in improving motor impairment in SCAs. However, since the reduced expression of BK channels and ion channels that serve as calcium sources for BK channels are tied directly to disease biology, targeting BK channels directly is the optimal strategy to target symptoms and disease progression. The current work makes major strides toward developing a potent lead molecule against the major target, BK. Interestingly, although BK-20 was inactive against SK channels, it was a potent inhibitor of Cav3.1, a calcium channel that serves as a potential calcium source for BK channel activation and whose expression is reduced in models of SCA1, SCA2, and SCA7 (Stoyas et al., 2019; Chopra et al., 2020; Bushart et al., 2021). Although not our initial intent, BK-20 could serve as a lead molecule to treat disorders with Cav3.1 gain-of-function mutations (Chemin et al., 2018) in which BK channel activation can improve Purkinje cell firing. Although unlikely to serve as a lead for treatment of firing abnormalities in SCA1 given its effects on Cav3.1, BK-20 does serve a valuable role, both as an improved positive control for future screens and in investigations of binding site analysis and channel activation for later structure-activity relationship work.

Future efforts will focus on expanding the primary screen to increase the number of chemical scaffolds for rational drug design and target validation of newer hits. The next phase of furthering these molecules will involve binding site analysis with orthogonal screens and mutagenesis and confirming compound activity in mouse behavioral studies. Additionally, we intend to explore pharmacological BK activation in combination with compounds that target other ion channels previously implicated in ataxia. Through these means, we will greatly progress toward meaningful therapies in spinocerebellar ataxias.

Acknowledgments

The authors would like to thank Dhananjay Yellajoshyula for support with cell culture and Vincent Groppi and Andrew Alt for discussions about the BK HTS. Research reported in this publication was supported by the Center for Chemical Genomics (CCG) at the University of Michigan Life Sciences Institute.

Authorship Contributions

Participated in research design: Srinivasan, Strassmaier, Wulff, Shakkottai.

Conducted experiments: Srinivasan, Huang, Chang, Nasburg, Nguyen, Strassmaier.

Contributed new reagents or analytic tools: Srinivasan, Strassmaier.

Performed data analysis: Srinivasan, Chang, Strassmaier.

Wrote or contributed to the writing of the manuscript: Srinivasan, Huang, Chang, Nasburg, Nguyen, Strassmaier, Wulff, Shakkottai.

References

Behrens R, Nolting A, Reimann F, Schwarz M, Waldschütz R, and Pongs O (2000) hKCNMB3 and hKCNMB4, cloning and characterization of two members of the large-conductance calcium-activated potassium channel β subunit family. *FEBS Lett* **474**:99–106.

Brenner R, Jegla TJ, Wickenden A, Liu Y, and Aldrich RW (2000) Cloning and functional characterization of novel large conductance calcium-activated potassium channel β subunits, hKCNMB3 and hKCNMB4. *J Biol Chem* **275**:6453–6461.

Bushart DD, Chopra R, Singh V, Murphy GG, Wulff H, and Shakkottai VG (2018) Targeting potassium channels to treat cerebellar ataxia. *Ann Clin Transl Neurol* **5**:297–314.

Bushart DD, Huang H, Man LJ, Morrison LM, and Shakkottai VG (2021) A chlorzoxazone-baclofen combination improves cerebellar impairment in spinocerebellar ataxia type 1. *Mov Disord* **36**:622–631.

Butler A, Tsunoda S, McCobb DP, Wei A, and Salkoff L (1993) mSlo, a complex mouse gene encoding "maxi" calcium-activated potassium channels. *Science* **261**:221–224.

Chemin J, Siquier-Pernet K, Nicouleau M, Barcia G, Ahmad A, Medina-Cano D, Hanein S, Altin N, Hubert L, Bole-Feysot C, et al. (2018) De novo mutation screening in childhood-onset cerebellar atrophy identifies gain-of-function mutations in the CACNA1G calcium channel gene. *Brain* **141**:1998–2013.

Chopra R, Bushart DD, Cooper JP, Yellajoshyula D, Morrison LM, Huang H, Handler HP, Man LJ, Dansithong W, Scoles DR, et al. (2020) Altered Capicua expression drives regional Purkinje neuron vulnerability through ion channel gene dysregulation in spinocerebellar ataxia type 1. *Hum Mol Genet* **29**:3249–3265.

Chopra R, Bushart DD, and Shakkottai VG (2018) Dendritic potassium channel dysfunction may contribute to dendrite degeneration in spinocerebellar ataxia type 1. *PLoS One* **13**:e0198040.

Dell'Orco JM, Pulst SM, and Shakkottai VG (2017) Potassium channel dysfunction underlies Purkinje neuron spiking abnormalities in spinocerebellar ataxia type 2. *Hum Mol Genet* **26**:3935–3945.

Dell'Orco JM, Wasserman AH, Chopra R, Ingram MAC, Hu Y-S, Singh V, Wulff H, Opal P, Orr HT, and Shakkottai VG (2015) Neuronal atrophy early in degenerative ataxia is a compensatory mechanism to regulate membrane excitability. *J Neurosci* **35**:11292–11307.

Durr A (2010) Autosomal dominant cerebellar ataxias: polyglutamine expansions and beyond. *Lancet Neurol* **9**:885–894.

Gribkoff VK, Starrett JE, Dworetzky SI, Hewawasam P, Boissard CG, Cook DA, Frantz SW, Heman K, Hibbard JR, Huston K, et al. (2001) Targeting acute ischemic stroke with a calcium-sensitive opener of maxi-K potassium channels. *Nat Med* **7**:471–477.

Huang S, Chen T, Suo Q, Shi R, Khan H, Ma Y, Tang Y, Yang G-Y, and Zhang Z (2021) BK channel-mediated microglial phagocytosis alleviates neurological deficit after ischemic stroke. *Front Cell Neurosci* **15**:683769.

Jayabal S, Chang HHV, Cullen KE, and Watt AJ (2016) 4-Aminopyridine reverses ataxia and cerebellar firing deficiency in a mouse model of spinocerebellar ataxia type 6. *Sci Rep* **6**:29489.

Kasumu AW, Hougaard C, Rode F, Jacobsen TA, Sabatier JM, Eriksen BL, Strøbæk D, Liang X, Egorova P, Vorontsova D, et al. (2012) Selective positive modulator of calcium-activated potassium channels exerts beneficial effects in a mouse model of spinocerebellar ataxia type 2. *Chem Biol* **19**:1340–1353.

Knaus H-G, Eberhart A, Glossmann H, Munujos P, Kaczorowski GJ, and Garcia ML (1994) Pharmacology and structure of high conductance calcium-activated potassium channels. *Cellular Signalling* **6**:861–870.

Kolski-Andreaco A, Lotfipour S, Bond C, Sailer C, Gunther-Knaus H, Leslie F, Adelman J, and Chandy KG (2007) SK channels modulate firing frequency, calcium influx, and stress-induced catecholamine secretion in mice. *FASEB J* **21**:A540 DOI: 10.1096/fasebj.21.5.A540-c.

Liang L, Li X, Moutton S, Vergano SAS, Cogné B, de Saint-Martin A, Hurst ACE, Hu Y, Bodamer O, Thevenon J, et al. (2019) De novo loss-of-function KCNMA1 variants are associated with a new multiple malformation syndrome and a broad spectrum of developmental and neurological phenotypes. *Hum Mol Genet* **28**:2937–2951.

Meera P, Wallner M, and Toro L (2000) A neuronal beta subunit (KCNMB4) makes the large conductance, voltage- and Ca2+-activated K+ channel resistant to charybdotoxin and iberiotoxin. *Proc Natl Acad Sci USA* **97**:5562–5567.

Miller JP, Moldenhauer HJ, Keros S, and Meredith AL (2021) An emerging spectrum of variants and clinical features in KCNMA1-linked channelopathy. *Channels (Austin)* **15**:447–464.

Olesen S-P, Munch E, Moldt P, and Drejer J (1994) Selective activation of Ca2+ -dependent K+ channels by novel benzimidazolone. *Eur J Pharmacol* **251**:53–59.

Raman IM and Bean BP (1999) Ionic currents underlying spontaneous action potentials in isolated cerebellar Purkinje neurons. *J Neurosci* **19**:1663–1674.

Sausbier M, Hu H, Arntz C, Feil S, Kamm S, Adelsberger H, Sausbier U, Sailer CA, Feil R, Hofmann F, et al. (2004) Cerebellar ataxia and Purkinje cell dysfunction caused by Ca2+-activated K+ channel deficiency. *Proc Natl Acad Sci USA* **101**:9474–9478.

Shakkottai VG, do Carmo Costa M, Dell'Orco JM, Sankaranarayanan A, Wulff H, and Paulson HL (2011) Early changes in cerebellar physiology accompany motor dysfunction in the polyglutamine disease spinocerebellar ataxia type 3. *J Neurosci* **31**:13002–13014.

Shakkottai VG and Fogel BL (2013) Clinical neurogenetics: autosomal dominant spinocerebellar ataxia. *Neurol Clin* **31**:987–1007.

Stoyas CA, Bushart DD, Switonski PM, Ward JM, Alaghatta A, Tang M-B, Niu C, Wadhwa M, Huang H, Savchenko A, et al. (2019) Nicotinamide pathway-dependent Sirt1 activation restores calcium homeostasis to achieve neuroprotection in spinocerebellar ataxia type 7. *Neuron* **105**:630–644.e9.

Strøbæk D, Teuber L, Jørgensen TD, Ahring PK, Kjær K, Hansen RS, Olesen SP, Christophersen P, and Skaaning-Jensen B (2004) Activation of human IK and SK Ca2+-activated K+ channels by NS309 (6,7-dichloro-1H-indole-2,3-dione 3-oxime). *Biochim Biophys Acta* **1665**:1–5.

Tseng-Crank J, Godinot N, Johansen TE, Ahring PK, Strøbaek D, Mertz R, Foster CD, Olesen SP, and Reinhart PH (1996) Cloning, expression, and distribution of a Ca(2+)-activated K+ channel beta-subunit from human brain. *Proc Natl Acad Sci USA* **93**:9200–9205.

Villalobos C, Shakkottai VG, Chandy KG, Michelhaugh SK, and Andrade R (2004) SKCa channels mediate the medium but not the slow calcium-activated afterhyperpolarization in cortical neurons. *J Neurosci* **24**:3537–3542.

Walter JT, Alviña K, Womack MD, Chevez C, and Khodakhah K (2006) Decreases in the precision of Purkinje cell pacemaking cause cerebellar dysfunction and ataxia. *Nat Neurosci* **9**:389–397.

Watase K, Weeber EJ, Xu B, Antalffy B, Yuva-Paylor L, Hashimoto K, Kano M, Atkinson R, Sun Y, Armstrong DL, et al. (2002) A long CAG repeat in the mouse Sca1 locus replicates SCA1 features and reveals the impact of protein solubility on selective neurodegeneration. *Neuron* **34**:905–919.

Weaver CD (2018) Thallium flux assay for measuring the activity of monovalent cation channels and transporters. *Methods Mol Biol* **1684**:105–114.

Weaver CD, Harden D, Dworetzky SI, Robertson B, and Knox RJ (2004) A thallium-sensitive, fluorescence-based assay for detecting and characterizing potassium channel modulators in mammalian cells. *J Biomol Screen* **9**:671–677.

Womack MD, Hoang C, and Khodakhah K (2009) Large conductance calcium-activated potassium channels affect both spontaneous firing and intracellular calcium concentration in cerebellar Purkinje neurons. *Neuroscience* **162**:989–1000.

Address correspondence to: Dr. Vikram G. Shakkottai, University of Texas Southwestern Medical Center, NL9.138A, 5323 Harry Hines Boulevard., Dallas, TX 75390. E-mail: Vikram.Shakkottai@UTSouthwestern.edu